

LPT Orsay 03-104
 UHU-FT/03-23
 FAMN SE-02/04

Evidences for instanton effects in Landau gauge lattice green functions.

Ph. Boucaud^a, F. De Soto^b, A. Le Yaouanc^a, J.P. Leroy^a, J. Micheli^a,
 O. Pene^a, J. Rodriguez-Guzmán^c, J. Quinteiro^c

^a Laboratoire de Physique Théorique¹

Université de Paris XI, Bâtiment 210, 91405 Orsay Cedex, France

^b Dept. de Física Atómica, Molecular y Nuclear

Universidad de Sevilla, Apdo. 1065, 41080 Sevilla, Spain

^c Dept. de Física Aplicada

Fac. Ciencias Experimentales, Universidad de Huelva, 21071 Huelva, Spain

Abstract

We present here striking evidences of the influence of instantons in the deep IR part of pure Yang-Mills gluon Green functions in the Landau gauge. We will propose a modified instanton field based on the Diakonov and Petrov variational method, whose accurate fit to our lattice results allows to gain information about the parameters of the Instanton liquid model (ILM).

1 Introduction

Confinement is a most challenging open problem in the strong interaction sector. It is a fundamental phenomenon which, nobody doubts, should follow from the QCD lagrangian, although this has not yet been really demonstrated. Understanding its mechanism would not only definitively establish QCD as the theory of strong interactions but would enrich and deepen our knowledge of one of the most difficult and most successful theories in physics.

An appealing approach to analytically understand some of the non-perturbative features of QCD is the evaluation of quantum fluctuations around topologically non-trivial classical solutions through the expansion of the path integral around

¹Unité Mixte de Recherche du CNRS - UMR 8627

these solutions. In fact these considerations are often generalized to configurations which are not exact solutions of the field equations but close to them and which we will name quasi-classical field configurations.

Famous examples of non-trivial solutions of classical equations of motion are instantons [1, 2]. Quasi-classical solutions considered in instanton liquid models [3, 4] (See ref. [5] for a good review on the subject) provide a successful connection between the instanton zero modes and the QCD chiral symmetry breaking [5]. More recently, instanton model predictions for quark-quark interaction seem to agree with QCD lattice results in the non-perturbative regime much better than those from Schwinger-Dyson equations (SDE) [6].

As a matter of fact, the methods like (ERG, SDE, ...) [7, 8], which basically follow down the renormalisation group flow from the large momentum to the small momentum one, present the risk of missing non-perturbative contributions which are negligible at large momentum but may play a dominant role at low momentum. If instantons or any other quasi-classical solutions have a deep influence over low energy dynamics, it seems not so surprising that SDE methods cannot recover them. In general, a dominance of instanton-induced effects on the dynamics of the QCD light-quark sector seems to emerge.

Although instantons have been first considered as a possible explanation of confinement [9], it is now generally accepted that they do not generate the area law for Wilson loops².

We have recently argued [10] that instantons, or instanton-like structures, have dramatic effects on the low momentum Green function in Yang-Mills theories and that they can explain the observed $\sim 1/k^4$ behaviour of the non-perturbative MOM strong coupling constant computed on the lattice.

Notice that this remark, not only advocates in favor of the presence of these quasi-classical structures in the lattice gauge configurations, but it also indicates that the quantum fluctuations do not contribute significantly to the Green functions in this momentum regime.

In the present paper we try a low momentum description of two- and three-gluon Green functions through Instanton liquid model (ILM) and would like to further elaborate on these features: what can we learn about the typical problem of these instanton-like structures, about their radius distribution? Why do quantum effects appear to be suppressed in this low momentum range? Has this some connection with confinement?

2 The QCD coupling constant: four regimes

We have presented in [10] a preliminary claim of instanton dominance at low energy, by analyzing in Landau gauge the following ratio of pure Yang-Mills

²A nother set of solutions of classical field equations, merons [11], has been recently reexamined as candidates to explain confinement [12].

Green functions:

$$s(k^2) = \frac{1}{4} \frac{G^{(3)}(k^2; k^2; k^2)}{(G^{(2)}(k^2))^3} Z_{\text{MOM}}^{3=2}(k^2) = \frac{k^6}{4} \frac{G^{(3)}(k^2; k^2; k^2)^2}{(G^{(2)}(k^2))^3}; \quad (1)$$

which is a non-perturbative MOM definition of the coupling constant, where $G^{(n)}$ is the gluon n -point correlation function and $Z_{\text{MOM}} = k^2 G^{(2)}$ is the gluon propagator renormalization constant in MOM scheme³.

In Fig. 1 we show on a log-log plot, that a roughly k^4 power law is satisfied by the lattice evaluations of $s(k^2)$, eq. (1), up to 0.8-0.9 GeV, for three different lattices, strongly supporting a quasi-classical description [10].

A very striking feature of results shown in Fig. 1, obtained with a low statistics of 20 configurations, is that there is a sharp transition at ~ 1 GeV between two regimes: below this scale $s(k^2)$ does not seem to fluctuate much and follows a smooth curve already with this small statistics and they comply to an instanton-like picture (the roughly k^4 power law), while above that scale the data suddenly deviate from the k^4 law and become much noisier: with the same statistics they do not show a smooth curve⁴. A tempting interpretation is that this statistical noise has to do with a strong influence of quantum fluctuations which increase suddenly above 1 GeV. We may understand this as follows: for a given profile and a given instanton radius, the ILM predicts no statistical fluctuation of the Green functions. The average over the instantons locations and their color orientation does not create any noise on Green functions which are translational and color rotation invariant. Only the dispersion (to be studied at length in this paper) of the instanton radius as well as varying effects of the neighbouring instantons produces some statistical noise. On the contrary the quantum contributions to Green function are generated by statistical fluctuations of the gauge fields around zero and Green functions appear as correlations in this statistical system.

Altogether we may distinguish four regimes:

Above 2.6 GeV we have shown [16] that the lattice data were dominated by perturbative QCD with a significant non-perturbative correction describable via OPE by the expectation value of A^2 . This means clearly a dominance of quantum fluctuations with small corrections from the A^2 condensate which may be generated by the quasi-classical solutions. Indeed the quasi-classical solutions, being large structures, are seen by the hard propagating gluons as an effectively translational invariant background. It is then easy to show that their dominant effect is amenable to an OPE treatment of the lowest dimension operator: A^2 [17].

Between 0.4 and 0.9 GeV the quasi-classical contributions dominate and the quantum effects are strongly depressed.

³We keep the name "coupling constant" for this well defined quantity although it could be argued that this name is not really appropriate in the low momentum regime.

⁴The smooth curve shown in fig 1(b) in [10] has been reached with 1000 configurations.

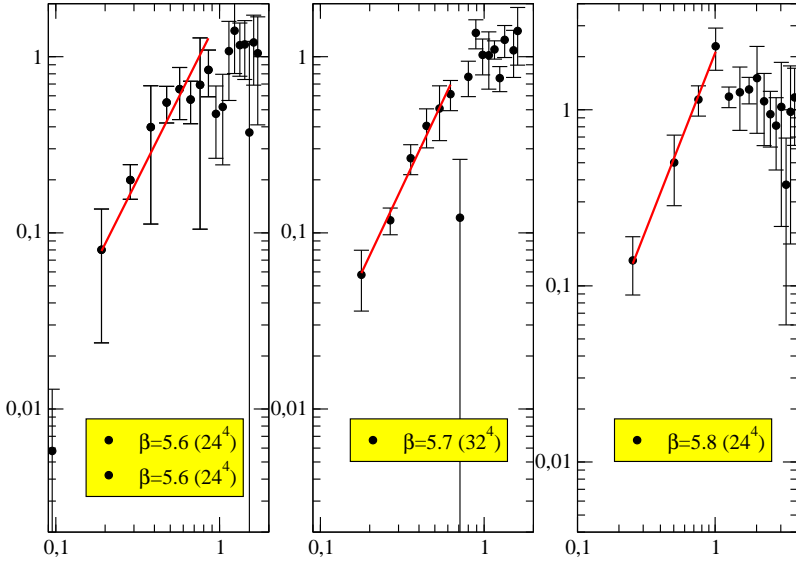


Figure 1: The low momentum k^4 behavior of $s(k^2)$ has been plotted for three different lattices ((5.6,24), (5.7,32), (5.8,24)), using 20 configurations, on log-log plots. Notice that above 1 GeV, no smooth line can be easily drawn joining the lattice data.

The 1 to 2.6 GeV region shows a strong quantum effect if only by the large statistical noise mentioned above. However, it is not at all describable in terms of perturbation theory. A description in terms of quantum fluctuations in a quasi-classical background should be tried. The latter background can no more be treated as simply as in the large momentum regime. Other non-perturbative effects may also play a role, for example related to confinement.

The very low momentum region below 0.4 GeV is still "terra incognita" and, being of the order of $2 = L$, (L being the lattice length) possibly strongly sensitive to finite volume artifacts.

3 A modified profile for the instanton-liquid model

In the following, we will try to describe the Green functions assuming that the relevant quasi-classical solutions are instanton liquids. Let us compute the quantity in eq. (1). We describe gluon fields in the low energy regime, a quasi-classical background dominance being assumed, as a superposition of instantons. In this framework, the gauge field in Landau gauge will be given by:

$$g B^a(x) = 2 \sum_i^X R_{(i)}^a - \frac{(x - z_i^j)}{(x - z_i^j)^2} \frac{j_k - z_i^j}{i} ; \quad (2)$$

where z^i (i) are the center (radius) of the instantons, $R_{(i)}^a$ is known as 't Hooft symbol, $R_{(i)}^a$ are color rotations embedding the canonical $SU(2)$ instanton into the $SU(3)$ gauge group, $i = 1; 3$ ($a = 1; 8$) is an $SU(2)$ ($SU(3)$) color index, and the sum is extended over instantons and anti-instantons.

The classical solution for an isolated instanton is the standard BPST one, $(\rho) = 1 = (\rho^2 + 1)$ [1]. Nevertheless, the superposition (2) is not a solution of Yang-Mills equations (as they are not linear), and we will treat below of a parameterization of the profile function inspired by an approximated minimization of the action for a finite density of instantons⁵.

The point here is that, just by assuming random color orientation and instanton position⁶, we obtain [10]:

$$\begin{aligned} g^2 G_{(I)}^{(2)}(k^2) &= \frac{n}{8} < {}^6 I(k^2)^2 > \\ g^3 G_{(I)}^{(3)}(k^2; k^2; k^2) &= \frac{n}{48k} < {}^9 I(k^2)^3 > \end{aligned} \quad (3)$$

where n stands for the instanton density, $< \dots >$ denotes average over the instanton radius for a given radius distribution (ρ) , normalized to 1, and where

$$I(s) = \frac{8}{s} \int_0^{\rho^2} dz J_2(sz) J_2(z) ; \quad s > 0 ; \quad (4)$$

J_2 being the second order Bessel J function. The factor g^n for n -points Green functions in l.h.s. of eq. l.h.s. of eq. (3) comes from the factor g in the l.h.s. of eq. (2).

Then, from Eq. (1),

$$s_{(I)}(k) = \frac{k^4}{18n} \frac{< {}^9 I(k^2)^3 >^2}{< {}^6 I(k^2)^2 >^3} : \quad (5)$$

As a first approximation, if we consider all instantons to have the same radius, we obviously obtain:

⁵The function ρ in eq. (2) is related to the function P in eq. (6) of ref. [10] by the relation $P(\rho^2) = 2(\rho) = x^2$

⁶This means that we neglect the color correlation which might exist, for example, between neighbouring instantons, an assumption which is usually done and which amounts to consider this instanton liquid as not being ordered.

$$\frac{\langle \mathcal{I}(k)^3 \rangle^2}{\langle \mathcal{I}(k)^2 \rangle^3} = 1; \quad (6)$$

and recover an exact k^4 -power law for any instanton profile.

In (6) the influence of the profile will only appear as a sub-leading contribution, that will also depend on the instanton radius distribution (See section 5.), while in (3) the leading contributions to the Green functions depend on the profile and will therefore be used by us to gain some understanding about the instanton radial shape and radii.

The variational D iakovov & Petrov equation.

If the QCD vacuum can be understood as an instanton liquid of finite density (See [5], for example), the BPSST profile will no longer be valid (it is only a zero density limit) especially at large distance from the instanton center where the overlap of neighboring instantons becomes important. Being interested in the low momentum regime we cannot neglect these effects.

A possible method to include the effect of instanton interactions, is to study the profile that minimizes the action of the instanton ensemble. Such a procedure was used in [4], where, through the Feynman variational principle, the equation

$$x^2 \frac{d^2}{dx^2} + 1 + \frac{\frac{2}{D_P} x^2}{4} - 3^2 + 2^3 + \frac{1}{6} \frac{C_{N_c}}{(\cdot)} = 0; \quad (7)$$

was obtained for the best profile, , eq. (6.7) in [4]. In the last term (\cdot) is just the usual renormalisation group -function evaluated at the instanton radius scale and C_{N_c} is a factor multiplying the instanton liquid partition function basically defined by the functional determinants in eq. (2.19) of [4]. This last term explicitly violates the apparent scale invariance of (7) and is hard to compute as it involves a functional derivative with its functional determinants. It is argued in [4] (discussion before eq. (6.1)) that one can neglect this last term provided the scale is fixed, e.g. by explicitly writing the profile as a function of $\frac{x}{r}$,

defining the instanton size through the condition $(1) = 1 = 2$. The argument goes grossly as follows. The classical equations are exactly scale invariant, and eq. (7) without the last term is indeed scale invariant. Scale invariance is broken in QCD by the quantum effects via the appearance of μ_{QCD} . The last term in eq. (7) is related to quantum effects (determinants) and this is why it generates the scale invariance breaking. In the zero density limit it produces the standard perturbative radius dependent instanton density $(\cdot) = \frac{5}{6} (\cdot)^6 e^{-(\cdot)^6}$ for $\mu_{QCD} = 1$ ⁷. It is furthermore assumed that it is the classical instanton

⁷An extension of this formula to large radii will be given in eq. (22).

interaction which dominates the large distance shape of the profile function. It is therefore legitimate, when interested in this behaviour, to neglect the details of this last term of eq. (7) provided we borrow from it a scale invariance breaking. This is done by a somehow arbitrary scale dependent constraint such as $(1) = 1=2$.

The parameter α_D ⁸ of eq. (7) represents on the contrary an average classical effect of the other instantons. It does not break scale invariance but it does enforce a squeezing of the instantons and therefore control the large x behaviour of $\langle x \rangle$. The parameter α_D is related to the instanton density, n . For example, for all the instanton with same radii [4]

$$\alpha_D^2, \frac{9N_c^2}{N_c^2 - 1} n \int_0^{\infty} dx^2 \underline{\langle x \rangle}^2 : \quad (8)$$

In fact eq. (8) is not really constrained by our lattice data as will be discussed later and we will not use it to determine α_D , but use eq. (7) to inspire a profile parametrization incorporating background-interaction effects.

The interesting limit of Eq. (7) is the one for $\underline{\langle x \rangle}$ (one should remember that is put by hand through the size-fixing condition), where not only the scale-invariance breaking term but the non linear one can be neglected because is expected to decrease at least as $\alpha_D^2 = x^2$. Then, eq. (7) becomes

$$x^2 \frac{d^2}{d\underline{\langle x \rangle}^2} + \underline{\langle x \rangle} \frac{d}{d\underline{\langle x \rangle}} - 4 + \alpha_D^2 x^2 \underline{\langle x \rangle} = 0 ; \quad (9)$$

which is a Bessel equation and we obtain

$$\underline{\langle x \rangle} = x K_2(\alpha_D \underline{\langle x \rangle}) \frac{e^{\alpha_D \underline{\langle x \rangle}}}{\underline{\langle x \rangle}} ; \quad (10)$$

where K_2 is the modified Bessel function of imaginary argument [9]. On the other hand, if $\alpha_D = 0$, the BPST profile is recovered, corresponding to the $n = 0$ limit. For finite n the $\alpha_D^2 x^2$ term becomes negligible for $x \gg 0$ where we also recover the BPST profile. For the sake of a simpler notation, we omitted to write any explicit dependence on the scale α_D (being completely rigorous, we had to write $\alpha_D(\underline{\langle x \rangle}; \alpha_D)$ and $_{BPST}(\underline{\langle x \rangle}) = \alpha_D(\underline{\langle x \rangle}; 0)$).

A possible parameterization⁹ of $\langle x \rangle$ inspired by (7), and incorporating these two limits, is:

⁸We have written the parameter with the subscript D , α_D , in order not to confuse it with the strong coupling constant α_s .

⁹In ref. [18], in the context of a constrained instanton model, the authors propose Ansätze to give account of large-scale vacuum field fluctuations also by matching similarly large and short distances limits of their constrained instanton equation. They also obtain solutions decaying exponentially at large distances.

$$\begin{aligned}
 \underline{\mathbf{x}}_j &= \frac{(\mathbf{D}_P)^2}{2} \frac{K_2(\mathbf{D}_P \mathbf{x})}{1 + \frac{(\mathbf{D}_P)^2}{2} K_2(\mathbf{D}_P \mathbf{x})} ! \stackrel{8}{\gtrless} \frac{x^2}{x^2 + 2} \text{ if } \mathbf{D}_P \mathbf{x} \neq 1 \\
 &\stackrel{8}{\gtrless} / K_2(\mathbf{D}_P \mathbf{x}) \text{ if } \mathbf{D}_P \mathbf{x} = 1
 \end{aligned} \tag{11}$$

which, although not being an exact solution of (7), satisfies both short and long distance limits. We will consider this in the following as our optimal choice for the profile function.

4 Green functions

The goal of this section is applying the parameterization in eq. (11) to fit our numerical results, obtaining thus \mathbf{D}_P and the instanton density. We start by writing the gauge field as the addition of a classical part, $B^a(\mathbf{x})$, and a quantum one, $Q_B(\mathbf{x})$, that in general depends on the classical background:

$$A^a(\mathbf{x}) = B^a(\mathbf{x}) + (Q_B)^a(\mathbf{x}); \tag{12}$$

then, for the two-point gluon Green function, we can write¹⁰:

$$hA^a(0)A^b(\mathbf{x})i = hB^a(0)B^b(\mathbf{x})i + h(Q_B)^a(0)(Q_B)^b(\mathbf{x})i; \tag{13}$$

or after Fourier transformation,

$$G_{\text{lattice}}^{(2)}(k^2) = G_{(I)}^{(2)}(k^2) + G_Q^{(2)}(k^2); \tag{14}$$

The working hypothesis we derive from the interpretation of g.1, is that in a certain region of momenta, say below 1 GeV, quantum effects are strongly suppressed and only classical properties are seen. Of course, we introduce this hypothesis based on a phenomenological observation, but it is not unconceivable that an intrinsically non-perturbative phenomenon like confinement could cause the disappearance of quantum correlations below the confining scale.

4.1 Estimated corrections to the instanton liquid model

From our data we have been led to fit the bare Green functions to the r.h.s of eq. (3) in a range $k_{\text{min}} < k < k_{\text{max}}$ without any correction. It is far from obvious that we can neglect either quantum corrections or lattice truncations of the quasi-classical model. This subsection is devoted to a justification of our choice which we present now, for the sake of clarity, at the price of having to anticipate on the results of some tests which will be detailed later.

¹⁰ Crossed terms vanish if the background corresponds to a local minimum of the action i.e. to a classical solution.

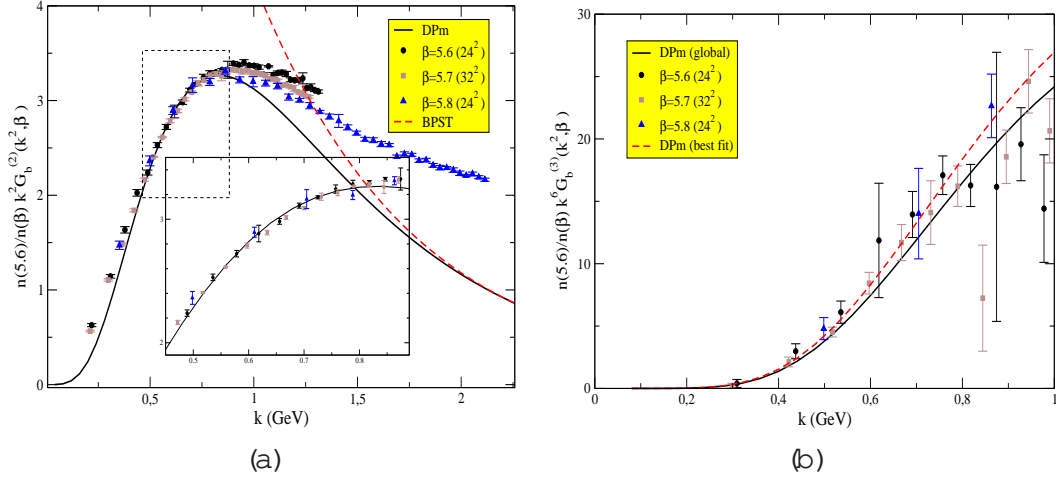


Figure 2: (a) We plot the gluon propagator, $k^2 G^{(2)}$, for the three lattices after a rescaling that matches data from $\beta = 5.7$ and $\beta = 5.8$ to those from $\beta = 5.6$. The dotted line is obtained from the BPST profile with $\beta = 0.3$ fm and the solid line is the best fit using our profile parameterization for gluon propagator. Clearly enough BPST cannot describe lattice data. (b) The points are lattice evaluations of symmetric vertex, $k^6 G^{(3)}$. The solid line is the best fit for the vertex with our profile parameterization, the density being required to be the same for both propagator and vertex, and the dotted is the best fit with a free density in the fit.

- (i) The Green functions $G^{(n)}$ estimated from three different lattice spacings match reasonably to each other, after a mere rescaling to a common value for some k_{\max} of the order of 1 GeV (see Fig. 2). These matching coefficients are close to 1, approximately in the ratios 0.95 / 1.0 / 1.05 for $\beta = 5.6; 5.7; 5.8$.
- (ii) It is difficult to know precisely what mechanism drives these matching coefficients slightly away from 1: quantum corrections, ultraviolet/infrared cutoffs on quasi-classical solutions. It is also impossible to know if these corrections are multiplicative, additive or of a more complex nature. The major lesson is that these corrections are small, and we decide for convenience to describe them by a multiplicative rescaling factor.
- (iii) This factor is defined as

$$G^{(m)}(k^2; a^{-1}) = \frac{G_{\text{lattice}}^{(m)}(k^2; a^{-1})}{G_{(I)}^{(m)}(k^2)}; \quad (15)$$

where a^{-1} is the regularization scale i.e. the inverse lattice spacing and $G_{(I)}^{(m)}(k^2); m = 2; 3$ are expressed in eq. (3). The functions $G^{(m)}(k^2; a^{-1})$ are $= 6^{11}$,

¹¹The factor $= 6 = 1/g^2$ comes from the factor g^2 in eq. (3).

n being the instanton density, are plotted up to an unknown global constant in g.3(a). $G_{(I)}^{(2)}(k^2)$ is here the best t to be discussed later. These plots show the good matching of different lattice spacings after a constant multiplicative rescaling has been performed (g.3(b) shows the result of this rescaling). They show a wide parabola having its minimum around $k = 0.65$ GeV. This minimum is around 7 to 8 which corresponds to the order of magnitude of the instanton density we will derive (the other factors being close to 1).

One possible explanation of this parabolic behaviour is an expected increase of quantum corrections towards larger k and, towards lower k , a relative increase of the ratio due to the fast decrease of the denominator in eq. (15): for example the fast increase at low k might be due to additive quantum corrections which are only visible when the quasi-classical background is very small. Additive corrections are anyhow necessary at $k = 0$ since the lattice data are non vanishing while the denominator of eq. (15) is zero. Whether this non vanishing of the lattice propagator at $k = 0$ is a finite volume effect violating Zwanziger's theorem, [26], will not be discussed in this paper since, as already mentioned, we restrain from discussing the finite-volume sensitive region below 0.4 GeV.

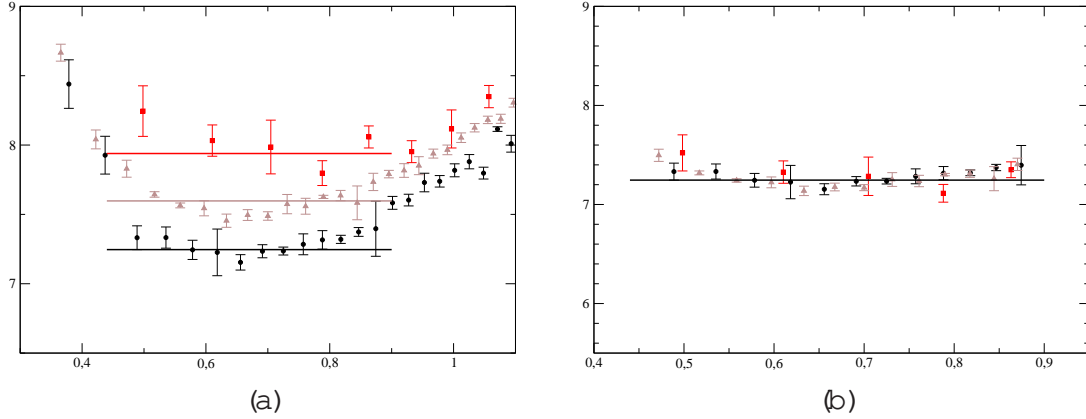


Figure 3: (a) We plot the ratios $n^{(2)}(k^2; a^2) = 6$ where n is the instanton density and a^2 is defined in eq. (15), for the three lattices, the squares, triangles and circles corresponding respectively to $a = 5.8$, $a = 5.7$ and $a = 5.6$. The horizontal axis represents the momentum in GeV. (b) The same points as in (a) but with the multiplicative rescaling performed. Different a^2 's coincide quite well, all show a parabolic type dependence in k .

(iv) If we stick to the momentum range plotted in g.3(b) these ratios do not deviate from a constant by more than a few percent. We will therefore per-

form our fits only in this range $k_{\text{min}} < k_{\text{max}}^{12}$ and approximate $^{(2)}(k^2; a^{-1})$ by a constant:

$$^{(2)}(k^2; a^{-1}) \quad k_{\text{min}}^2 < k^2 < k_{\text{max}}^2 \quad (16)$$

(v) Since from g. 3(a) the different $^{(2)}(a^{-1})$ differ also by no more than a few percent we decide to take from now on all these $^{(2)}(a^{-1})$'s as equal at the cost of an expected discrepancy between the fitted densities of a few percent. We take

$$8a^{-1}; \quad ^{(2)}(a^{-1}) = ^{(2)}a^{-1}(5:6) : \quad (17)$$

where $a^{-1}(5:6)$ is the inverse lattice spacing for $\tau = 5:6$.

(vi) We now wonder if the hypothesis eq.(17) can be extended to the coefficients $^{(3)}(a^{-1})$. The small dependence on k and on a^{-1} can be seen, although with larger errors, in g. 2(b) where the different lattice data seem to fit one common solid curve representing the model. The next question is the validity of the hypothesis

$$^{(3)}(a^{-1}) = ^{(2)}(a^{-1}): \quad (18)$$

To test the hypothesis $^{(3)} = ^{(2)}$ we look at g.4. The vertical axis corresponds to the ratio $^{(3)}(a^{-1}(5:6)) = ^{(2)}(a^{-1}(5:6))$ or equivalently to $n^{(3)} = n^{(2)}$ where we define $n^{(m)} = n^{(m)}(a^{-1}(5:6))$, n being the instanton density. The horizontal axis corresponds to the instanton radius r , supposed to be the same for all instantons. For that instanton radius a best fit of the bare Green functions is performed according to the formula:

$$G_{\text{lattice}}^{(m)}(k^2; a^{-1}) = G_{(I)}^{(m)}(k^2) \quad (m) \quad (19)$$

with $G_{(I)}^{(m)}(k^2)$ given by eq. (3). The plot 4 shows for each m an agreement between different r 's which is a surprise: it tells that the ratio $^{(3)}(a^{-1}) = ^{(2)}(a^{-1})$ is almost independent of the lattice spacing even though it does strongly depend on r . The dotted curve shows the r^2 of the common fit to $G^{(2)}$ and $G^{(3)}$. The smallest r^2 corresponds to a ratio $^{(3)}(a^{-1}) = ^{(2)}(a^{-1})$ ranging from 0.8 to 0.9, i.e. close to 1. This also corresponds to a value of the radius around 0.3 fm which is the one favored by phenomenology. This leads us to consider eq. (18) as quite reasonable.

¹²To be precise our fits use the window $k_{\text{min}} = 0.44$ and $k_{\text{max}} = 0.89$.

(vii) All the arguments up to now have shown an approximate equality to a few percent of all $^{(m)}(a^{-1})$'s. We are left with an unknown global constant. The fact that these factors are so close to each other suggests that the corrections to the instantonic contribution (whatever their origin may be) are small. It is then natural to expect that these correction factors are also close to 1. This is confirmed by a result which will be detailed at the end of this paper via the following argument: if we initially take $^{(2;3)} \notin 1$, apply MOM renormalisation and then eq. (1), we obtain:

$$_{\text{Latt}}(k) = \frac{k^6}{4} \frac{G_{\text{Latt}}^{(3)}(k^2; a_{\text{Latt}}^{-1})^2}{G_{\text{Latt}}^{(2)}(k^2; a_{\text{Latt}}^{-1})^3} = \frac{^{(3)}(a_{\text{Latt}}^{-1})^2}{\underbrace{^{(2)}(a_{\text{Latt}}^{-1})^3}_{\{Z\}}} \quad (20)$$

where the term above the curly bracket in the r.h.s. introduces a supposed-to-be-sub-leading correction, depending on the regularization parameter, that we neglect in our analysis for the present work (and did the same in [10]). Let us anticipate a little. The reasonable agreement between the instanton density obtained from the coupling constant $_{\text{Latt}}(k)$ in table 3 with the one in table 1 implies a ratio $(^{(3)})^2 = (^{(2)})^3$ close to 1. Combined with $^{(2)} = ^{(3)} = 1$ presented in the preceding item ends up with an approximate justification of our hypothesis that all $^{(n)}(a^{-1}); n = 2; 3 = 1$ for all 's in the range considered here and justify our assumption:

$$^{(m)}(k^2; a^{-1}) = 1 \quad \text{for } m = 2; 3 \quad \text{and} \quad k_{\text{min}} < k < k_{\text{max}}: \quad (21)$$

with $k_{\text{min}} = 0.44 \text{ GeV}$ and $k_{\text{max}} = 0.89 \text{ GeV}$.

4.2 Numerical results.

The numerical data that we shall exploit all over the paper result from two simulations on a 24^4 lattice with bare coupling constants given by $\beta = 5.6$ and $\beta = 5.8$, and a simulation on a 32^4 lattice for $\beta = 5.7^{13}$, in the Landau gauge. We calibrate all these simulations with the ratios of lattice spacings for different 's given in ref. [13] and $a_{\text{Latt}}^{-1}(\beta = 6.0) = 1.97 \text{ GeV}$ (this last value was used in ref. [14] in consistency with the very precise measurement of the lattice spacing with a non-perturbatively improved action in ref. [15]).

Coefficients in [13] are fitted for $\beta = 6.0$. In this work, we make use of rather low values $\beta < 6.0$, in order to have larger volumes. These low values of β show for the quantity χ a good scaling with results at $\beta = 6.0$, a signal

¹³With the two lattices for $\beta = 5.6; 5.7$ we simulate practically the same physical volume and are thus in position to check lattice spacing artifacts.

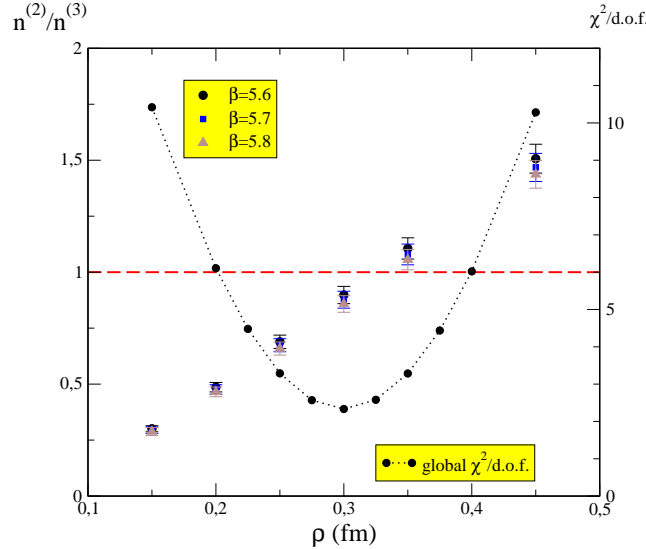


Figure 4: We plot the ratios $n^{(3)} = n^{(2)}$ where we define $n^{(m)}$ as $a^{-1} (5:6)$, n being the instanton density. These are fitted from two-point and three-point Green functions for a fixed value of instanton radius, ρ , represented on the horizontal axis. The dotted line joins the optimal $\chi^2/\text{d.o.f.}$ (on left y-axis) as a function of the radius.

that these lower β 's give reasonable results. The risk with these simulations is the extrapolation needed to calibrate the lattice spacing, that might be a non-negligible source of systematic error in our measures.

(fm)		0.2	0.25	0.3	0.35	0.4
n (fm ⁻⁴)	= 5:6	26.5(1)	13.18(5)	7.75(3)	5.12(2)	3.63(1)
	= 5:7	27.2(1)	13.54(5)	7.98(3)	5.28(3)	3.76(2)
	= 5:8	27.8(2)	13.9(1)	8.20(7)	5.41(4)	3.86(3)
DP		0.393(2)	0.527(2)	0.675(2)	0.836(3)	1.005(3)
$\chi^2/\text{d.o.f.}$		6.1	3.3	2.3	3.3	6.0

Table 1: Best-fit parameters for several fixed instanton radii. The two- and three-point Green functions are fitted simultaneously with the same instanton density. Note that stated errors are only statistical.

We collect the results of our fits for several fixed instanton radii in tab.1. An instanton density, although the same for both Green functions¹⁴, is independently fitted for each particular lattice spacing. We look thus for a remnant of a sub-leading dependence on the regularization parameter. The careful reader may

¹⁴Notice the difference with the fits presented in fig. 4 where different densities are assumed for $G^{(2)}$ and $G^{(3)}$.

have noticed that the relative density splitting between different β 's is slightly smaller (3 % for $\beta = 0.1$) than the splitting between the linear fits in g_3 (4.5 %). This is due to the factor g^2 in eq. (3) (about 1.5 %).

Crudeness of our quasi-classical approximation.

It is worth to repeat here that our fits rely on the crude approximation eq. (21) which is not valid at more than a few percents as discussed at length in subsection 4.1. This is the origin of the difference between the densities in tab. 1. This is also the reason why the minimal χ^2 -d.o.f. in table 1 is of the order of two because we force the overall factor to be the same in fits for both two- and three-point Green functions. This tells about the crudeness of completely neglecting the sub-leading contributions from quantum fluctuations and lattice truncation of the classical solutions. Much better matchings might have been obtained had we relaxed the constraint eq. (21). We refrained from doing so because it would have needed additional input about quantum fluctuations and lattice truncation of classical solutions which would have been mere guesses and wouldn't have yielded any stronger evidence.

At the present stage of the work, the best we can do is to assume eq. (21) and get what we believe to be a fairly coherent description of our whole set of lattice data. The best-fit parameterization in Tab. 1 is the best we can achieve, and it is not that bad, although we know that the density obtained there is affected roughly by a 20% of systematic uncertainty¹⁵.

5 The effect of the instanton radius dispersion

We have performed satisfactory enough and independent fits for the three different lattices from s to the k^4 -formula, eqs. (5, 6), and obtain the estimates for the instanton density shown in the central column of Tab. 2. They differ by about 25 % from the profile dependent ones obtained from $G^{(m)}$ and presented in table 1. The fit of s is done on a rather firm ground since, contrarily to the fits of $G^{(m)}$, the prediction does not at all depend on the profile neither on the radius but only on eq.(6), of course on the hypothesis that the radius distribution is a delta function i.e. that all the radii are equal. s is therefore the best quantity to estimate the corrections to this rather drastic hypothesis. If the k^4 law does not depend on the instanton profiles but only on the β -function profile, the corrections do¹⁶.

We will present now some preliminary estimations of these corrections using what has been learned in the preceding sections. This will allow us to estimate if

¹⁵This uncertainty is estimated from the $n^{(3)} = n^{(2)}$ ratio at the minimum χ^2 in fig. 4, ranging around 0.8–0.9 instead of 1

¹⁶Obviously the influence of the radius distribution (s) will not be independent of the profile (Remember (3)).

these corrections are small enough to legitimate the assumption of equal radii as a first approximation. Second we can check these corrected s against data and thus confirm or invalidate the whole approach.

We will proceed as follows. We will first estimate from a reasonable radius distribution and from profile functions already discussed the expected form of the Green functions corrected for this non-delta distribution. The $s(k)$ will be approximated in our fitting window by a simple ck^d/n function, n being the instanton density, c and d being calculated from both the radius distribution and the instanton profile function. In a second step the same functional form ck^d/n will be fitted on our lattice data. From the t , knowing c from this theoretical work, we derive n (to be compared to previous estimates) and d which is compared to the theoretical prediction.

We first need an estimate of the radius distribution. The one-loop computation for the tunneling amplitude of classical minima in gauge theories gives the standard growth $(\rho) \sim t^6$ for instanton radii distribution [2]. On the other hand, the classical interaction of instantons in the background have to introduce small-distance repulsion that strongly suppress large instantons and leads to a well-behaved partition function [5].

Applying the Feynman variational principle, Diakonov & Petrov found indeed that this infrared growth is balanced as follows [4]:

$$(\rho) = 2 \frac{\frac{2}{7} \overline{d}^2}{(7=2)} \sim 6 \exp \left(-\frac{7}{2} \overline{d}^2 \right); \quad (22)$$

where $\overline{d}^2 = \int_0^{R_1} d^2 \rho(t)$ and $\Gamma(n) = \int_0^{\infty} dt e^{-t} t^{n-1}$ is the standard Euler's gamma function.

The BPST profile.

The first natural approximation step is to use the profile function from the BPST solution, $(\rho) = \sqrt{2} = (x^2 + \rho^2)$, and thus neglect the effect of neighbouring instanton's classical interaction. The IR behavior of gluon Green functions for this profile is:

$$\begin{aligned} G_{(I)}^{(m)}(k^2) &= \frac{k^2}{m} \frac{n}{2^{2m-2}} \frac{1}{6} \sum_{r=1}^{m=2} \frac{(-1)^{r+1}}{r} \frac{3^m}{m} I(k^2)^m > \\ &= n \frac{4k^2}{m} - \frac{4}{6} \frac{k^2}{k^4} \end{aligned} \quad (23)$$

$$\begin{aligned}
 & \text{for } k = 1 \\
 & 1 + O\left(\frac{7}{2^2 k^2}\right) \quad \text{for } k = 1 \\
 & \frac{\left(\frac{7+2m}{2}\right)}{4^m} \left(\frac{7}{2}\right) \quad \frac{2}{7} k^2 \quad m \quad 1 + b_m (k^2) \frac{2}{7} k^2 + O\left(\frac{2}{7} k^2\right)^2 \quad \text{for } k = 1
 \end{aligned}$$

where $g = 6 = g_{\text{Latt}}^2$ is the lattice parameter for the bare coupling and

$$b_m(k^2) = \frac{m(7+2m)}{16} 2_E \frac{3}{2} + \frac{9+2m}{2} + \ln \frac{2}{7} k^2 \ln 4 : (24)$$

where γ is the Euler constant ($0.577216\dots$) and $(z) = \gamma(z) = (z)$ the Euler's digamma function. The first correction to the low momentum k^4 behavior of the quantity (1), is then given by:

$$_s(k) = \frac{121}{1134 n} k^4 - 1 + \frac{6}{56} \overline{k^2} k^2 - 2 \ln \frac{\overline{k^2}}{56} + \frac{22567}{3465} + \dots \quad (25)$$

valid for $\bar{k}^2 \ll 7=2$.

It is more convenient for further analysis to approximate the prediction for $s(k)$ from eq. (22) and BPST profile, (with $\tau = \frac{1}{2} = 1.5 \text{ GeV}^{-1} = 0.3 \text{ fm}$ from table 1) by the functional form: $c = (18/n) (k/(1 \text{ GeV}))^d$. We perform this numerically in the window $(0.3 \text{ to } 0.9) \text{ GeV}^{17}$ and obtain

$$s(k), \quad \frac{1:37}{18 \text{~n}} \quad \frac{k}{1 \text{GeV}} \quad : \quad 3:75 \quad (26)$$

Our D-P inspired problem.

We compute now the same averages with our optimal procedure parameterized in eq. (11) of section 4 and obtain the low-momentum ($k \ll D_P$) prediction for Green functions:

$$G_{(I)}^{(m)}(k^2) = n \frac{r}{6} \frac{2^2}{7^2} \frac{!}{D_P^2} \frac{\frac{7}{2} + m}{\frac{7}{2}} \frac{4k^2}{m} 1 + O \frac{2}{D_P^2} ; k^2 \frac{!}{2} \quad : \quad (27)$$

¹⁷ This window is slightly larger than our lattice window (0.44–0.89) GeV. The question here is the validity of approximating eqs (23,24) by a power law which is shown to extend further than our lattice fitting window.

The result equivalent to eq. (26) for this profile, using the same fitting procedure over the same window, with a phenomenological radius $\bar{r} = \frac{r}{2} = 1.5$ GeV and $\alpha_D = 0.675$ from table 1, is

$$s(k) \sim \frac{1.45}{18 n} \frac{k}{1 \text{GeV}}^{3.83}; \quad (28)$$

The parameters α_D and \bar{r} have not been fitted here but taken from the fits in table 1 which were performed assuming the same profile but a delta radius distribution. However we have also checked that fitting the product $\alpha_D \bar{r}$ with the radius distribution eq. (22) induces a negligible change of 3 %.

The calculations using BPST and DP-inspired profiles end-up with rather similar conclusions, eqs. (26,28): with respect to the fixed radius assumption, eqs. (5,6), the prefactor $1/18$ is enlarged by around 40 %, while the exponent 4 is slightly reduced.

Lattice results

We first present in this subsection, collected in next tab.2, the results for the density obtained, for our three lattice data set, through the fit of the MOM QCD coupling constant defined in eq. 1) to the k^4 -power law in eqs. (5,6).

Lattice	$n (\text{fm}^{-4})$
5.6 (24^4)	5.2 (6)
5.7 (32^4)	6.7 (4)
5.8 (32^4)	6 (1)

Table 2: Results for the density obtained from fitting lattice coupling constant to eqs. (5,6) i.e. assuming a k^4 behavior. Errors quoted are only statistical and computed by jackknife method

Then, we include in tab. 3 the results for the best fits of the same QCD coupling constant lattice data to a power formula of the type of eq. (28) using the prefactor $1.45 = (18 n)$ but leaving the power of k free to be fitted altogether with the density.

We use for both the same fitting window, $0.44 < k < 0.89$, used in section 4 to obtain the best profile parameterization. Densities in tab.3 are systematically larger than in tab. 2 because of the factor ' 1.45 in front of the power on k in eq. (28)¹⁸. However, all these estimates are in the right ballpark as far as different arguments[20] seem to point towards an instanton density of a few fm^{-4} 's. The $\chi^2/\text{d.o.f.}$'s in tab. 3 are ridiculously tiny. This may be due to (i) the strong

¹⁸Such a factor is similar in eq. (26) where we assume a BPST profile. It is larger than one, which tends to compensate for the power smaller than 4.

Lattice	$n (\text{fm}^4)$	power	$\chi^2/\text{d.o.f.}$
5.6 (24^4)	8 (2)	3.8 (4)	0.068
5.7 (32^4)	10 (3)	3.9 (5)	0.36
5.8 (24^4)	7 (1)	3.8 (6)	0.007

Table 3: The same that in tab. 2 but here fitting to eq. (28) except for the power on k , taken to be free. The third row shows the $\chi^2/\text{d.o.f.}$ The fitted powers are lower than 4 but the errors show that the power 4 is not excluded by our fits.

correlation of our lattice estimates of the coupling for the different momenta, all computed from the same set of gauge field configurations¹⁹. (ii) the small number of points in our fitting window (only 3 for $5.8(24^4)$).

The best-fit parameters computed lattice by lattice in tab. 3 manifest no appreciable systematic deviation²⁰. A global fit for the whole set seems thus to be appropriate. The resulting power deduced from a global fit is:

$$3.91 \quad 0.45 ; \quad (29)$$

which is compatible with eqs. (26,28), but also with a k^4 -power law. The $\chi^2/\text{d.o.f.}$ is 0.39 for this global fit. In ref. [10], the same global fit was performed for more lattices (we added estimates of s over smaller volumes and larger $'s$: $5.7(24^4)$, $5.9(24^4)$, $6.0(24^4,16^4)$); these, having only one point inside the fitting window, have been discarded from the present work. The result of the latter analysis was 3.82 (8) as best-fit for the power. The error was there clearly underestimated²¹ but the evaluations of the coupling constant from larger $'s$ do not practically affect the central value. This fact indicates that exploiting the small $'s$ used in the present work does not seem to introduce any sizable bias, at least over the low-momentum region, on the determination of s .

The fitted power being close to 4 legitimizes our initial hypothesis of neglecting, in first approximation, the influence of the radius distribution on the direct description of Green functions which yielded a probe-independent determination of $s(k)$. Only as a second approximation, when the radius dispersion is considered, does the probe function play a role which mildly corrects the k^4 -power law and a more significant correction to the prefactors.

One comment about eq. (8) is in order to close this section. If we take in the l.h.s. the value of χ^2_{DP} fitted from our lattice data and in the r.h.s. our optimal

¹⁹Still, our jackknife estimate of the statistical error is reliable because, if the global average for the different momenta are correlated the averages for different sets of gauge configurations are not.

²⁰As we expect once we have found the sub-leading lattice spacing dependent corrections in eq. (20) to be small.

²¹We used the criterium of assuming one standard deviation as $\chi^2 = \frac{2}{m_{\text{bin}}} + 1$, which is biased by the strong correlations between data for different momenta as just discussed.

profile function eq. (11) fitted on our lattice data, we obtain an instanton density of the order of 1 fm^{-4} , i.e. one order of magnitude smaller than the fits in tab. 3. What does this mean? Our interpretation is that eqs. (7,8), derived from the instanton liquid model through a variational procedure, gives only a rough solution of the instanton liquid dynamics, and should be used as a semi-quantitative scheme of what is going on. In particular it should be stressed that the integral in eq. (8) is strongly dependent on the behaviour at infinity of the profile function and would even diverge for the BPST profile. This drastic sensibility of eq. (8) to the profile has to be opposed to the close similarity of eq. (26) and eq. (28). We feel therefore much safer using the latter equations and our lattice data than using eq. (26).

6 Discussions and Conclusions

6.1 Comparison with the Schwinger-Dyson equations' predictions

The infrared behaviour of gluon and ghost correlation functions in Landau gauge QCD has been largely studied within the Schwinger-Dyson equations (SDE) formalism. After assuming ghost dominance, one unique exponent, ζ , determines the leading long-range behavior of both gluon and ghost propagator. In particular,

$$G_{\text{SD}}^{(2)} \sim k^{2-1}; \quad (30)$$

where general arguments seem to establish that $0 < \zeta < 1$ [21]. Several truncation schemes, with different degrees of sophistication, have been employed to solve SDE for gluon and ghost propagators and obtain critical exponents such as $\zeta = 0.92$ [21, 22], $\zeta = 0.77$ [23] or $\zeta = 1$ [24]. The authors of ref. [8] claim that they correct previous mistakes and give a better result: $\zeta = 0.595$. Moreover, $\zeta = 1/2$ is derived from the proximity of the Gribov horizon in infrared directions in ref. [26].

In the previous section, we computed the gluon propagator in the low momentum regime, in our instanton approach, and obtain

$$G_{(I)}^{(2)} \sim \begin{cases} k^2 & \text{for BPST} \\ k^2 & \text{for DP} \end{cases} \quad (31)$$

We have already noticed, see figs. 2 and 3 that our instanton description fails to reproduce lattice data for very low momentum and that some corrections are seen.

It is nevertheless instructive to compare the prediction for α_s from our preferred purely instantonic description with SD. An interesting remark is that, using the BPST profile to describe the instantons solutions of the classical background we reproduce the lower bound given by SD, $\alpha_s = 0$. As a matter of fact, the BPST profile decreases as $x \rightarrow 1$ slower than any other more realistic profile and generates thus a prediction for the gluon propagator with a stronger divergence as $k \rightarrow 0$. Our DP inspired profile for background instanton solutions, eq. (11), decreasing for large distances as given by eq. (10), leads to predict $\alpha_s = 1$, i.e. the upper limit given by SDE, however much larger than the last SDE prediction of [8] of $\alpha_s \approx 0.595$. The Gribov horizon condition is thus satisfied by DP inspired profile, although the requirement of a positive measure in the Fadeev-Popov formalism does not seem to be connected with eq. (7).

In [25] it is claimed that the infrared exponent γ is dependent on the details of the truncation, and the value $\gamma = 0.5$ is chosen in view of the good agreement with lattice results. Indeed, the observation that $G_{\text{lattice}}^{(2)}(0)$ is a finite non-vanishing constant if it remains valid in the infinite volume limit, favors $\gamma = 0.5$.

The comparison with the SDE prediction deserves further study. As we have already mentioned we would like to question to what extent the SDE formalism can account for semi-classical structures which are very strongly suppressed at large momenta, where the initial conditions for the SDE are tuned. This is partly accounted for by the attempts to match at large momentum the effect of the A^2 condensate via OPE.²²

6.2 Conclusions

The claim of this paper is the dominance of the quasi-classical gauge fields configurations over low energy dynamics in the pure Yang-Mills sector of QCD. We have given a reasonable framework to understand gluon two- and three-point Green functions based on QCD instantons. In a previous paper [10], we had shown a k^4 dependence of the coupling constant in MOM scheme, which gave us a rather clean indication of the dominance of semi-classical solutions over low energy QCD dynamics, and some indication that these solutions might be instantons.

In order to go further in the understanding of this very remarkable feature, we tried here a direct description of gluon Green functions in this framework. In order to achieve this, contrarily to what happens for the MOM coupling constant, the knowledge of the instanton profile is mandatory. The single-instanton BPST profile clearly fails to describe the low momentum behavior since it predicts a divergent gluon propagator for $k \rightarrow 0$ in full contradiction with the lattice results. This is understood as an effect of the deformation of instantons far from their centers due to the influence of other instantons. Indeed, The BPST singularity of the gluon propagator is corrected when effects of instanton interactions are taken

²²We thank Akihiro Shibata for this remark.

into account through a parameterization of the profile derived from variational methods [4], and it leads to a successful description of the low momentum behavior of lattice two- and three-point Green functions. When we say "instanton-like structures" we also mean that we cannot at this point exclude, for example, a significant amount of monopoles [1, 12] which would of course modify our density estimates.

We fit our lattice data for the Green functions in an instanton liquid model (ILM), below energies of 0.9 GeV , and above 0.4 GeV . Below 0.4 GeV we have too few lattice data and furthermore the lattice computed gluon propagator gives a non null value for the $k \rightarrow 0$ limit, contradictory to the expectation of an ILM. Third quantum corrections to the semiclassical solutions should be more visible when the latter vanish. Last but not least, this region is expected to be strongly finite-volume sensitive and deserves a special study.

Our measured densities (See tab. 2,3), while in the ballpark of lattice estimations, give a contribution to the gluon condensate $g^2 G^{a/2} = 4 \text{ GeV}^4 (1400 \text{ MeV})^4$ for $n = 8 \text{ fm}^{-4}$, significantly larger than other estimates, based on QCD sum rules [27], $g^2 G^{a/2} = 0.5 \text{ GeV}^4 (840 \text{ MeV})^4$, or more recently [28], $g^2 G^{a/2} = 0.9 \text{ GeV}^4 (970 \text{ MeV})^4$. Some discrepancy between the pure Yang-Mills condensate and the one from QCD sum rules is not unexpected: in ref. [29] (see eq. (106)) it is argued that light dynamical quarks might reduce the G^2 condensate by a factor 2 to 3. Furthermore, the QCD sum rules are not so accurate neither our density estimates which, for instance, would be modified by the presence of other "instanton-like structures" or instantons deformations.

Altogether our density estimate is close to the maximum acceptable: with a density of 8 per fm^{-4} the average distance between two neighbouring instanton centers is of the order of 0.6 fm i.e. twice the average radius, a really dense packing.

We have discussed the effect of the instanton radius dispersion. We find a subdominant but non negligible influence of the radius dispersion on the coupling constant: We find that a coherent description of both two- and three-point Green functions only emerges when the instanton radius reaches the vicinity of $1/3 \text{ fm}$, that is the value derived from phenomenological arguments. Furthermore, after invoking a radius distribution obtained from DP's variational methods [4], we correct the previously predicted k^4 -power followed by $s(k)$ by a slight reduction of the power ($k^{3.83}$) and a 40 % increase of the prefactor. The fits of all our lattice data to a free-power law on k always produces a best-fit exponent lower than 4 but statistically compatible with 4 (We obtain 3.91(45) from a global fit combining all our lattice data sets). This seems to confirm the trend predicted from radius distribution, but the small number of points in the region of interest and the big errors lead to a large uncertainty that prevents us from a more conclusive statement. Once this radius dispersion is considered we get a good agreement of the density derived directly from a fit of the two- and three-point

Green functions and a fit to $s(k)$.

The lattice spacings used in this study have been chosen rather large since we wished to reach low momenta with a not too large number of lattice points. It might be feared that these values are too far from the continuum limit, too much in the strong coupling regime, to be reliable. We did not see any sign of a non-smooth dependence of any quantity on the lattice spacing. However, for safety, it is advisable (and under progress) to follow-on these studies at, say, $a = 6.0$ with as large a physical volume as used here. Larger statistics and larger physical volumes at a given lattice spacing are also needed.

The lattice gluon propagator at (or close to) $k \neq 0$, has also open problems, for example in relation to the Zwanziger problem [26] and critical exponent in relation to instantons. Other theoretical questions are pending such as the reason why quantum fluctuations only play a sub-leading role in this momentum range²³. Still we believe that we have given a series of rather convincing evidences of the influence of instanton-like structures on the low energy QCD and more precisely on the low momentum behavior of gluon Green functions.

References

- [1] A. A. Belavin, A. M. Polyakov, A. S. Shvarts and Y. S. Tyupkin, Phys. Lett. B 59, 85 (1975).
- [2] G. 't Hooft, Phys. Rev. D 14, 3432 (1976) [Erratum -ibid. D 18, 2199 (1978)].
- [3] Shuryak E. V., Nucl. Phys. B 198 (1983) 83; Ilgenfritz E. M., Mueller-Pfeusser M., Nucl. Phys. B 184 (1981) 443.
- [4] D. D. Diakonov and V. Y. Petrov, Nucl. Phys. B 245, 259 (1984).
- [5] T. Schafer and E. V. Shuryak, Rev. Mod. Phys. 70 (1998) 323 [arXiv:hep-ph/9610451].
- [6] P. Faccioli and T. A. Degrard, arXiv:hep-ph/0304219.
- [7] R. A. Ikofer and C. S. Fischer, arXiv:hep-ph/0309089 and references therein.
- [8] C. Lerche and L. von Smekal, Phys. Rev. D 65 (2002) 125006 [arXiv:hep-ph/0202194]; R. A. Ikofer, C. S. Fischer and L. von Smekal, Eur. Phys. J. A 17 (2003) 773 [arXiv:hep-ph/0209366]; C. S. Fischer and R. A. Ikofer, Phys. Lett. B 536 (2002) 177 [arXiv:hep-ph/0202202].
- [9] A. M. Polyakov, Phys. Lett. B 59, 82 (1975).
- [10] P. Boucaud et al., JHEP 0304, 005 (2003) [arXiv:hep-ph/0212192].

²³If we naively add quantum and classical contributions to the gluon propagator (Eq. (13)), the perturbative quantum contribution would diverge

[11] C . G . Callan, R . F . D ashén and D . J . G ross, Phys. Lett. B 66 (1977) 375.

[12] F . Lenz, J . W . Negele and M . Thies, arX iv:hep-th/0306105.

[13] M . Guagnelli, R . Petronzio, J . Rolf, S . Sint, R . Sommer and U . Wol [ALPHA Collaboration], Nucl. Phys. B 595 (2001) 44 [arX iv:hep-lat/0009021].

[14] D . Becirevic, P . Boucaud, J . P . Leroy, J . M icheli, O . Pene, J . Rodriguez-Q uintero and C . Roiesnel, Phys. Rev. D 60 (1999) 094509 [arX iv:hep-ph/9903364]; Phys. Rev. D 61 (2000) 114508 [arX iv:hep-ph/9910204].

[15] D . Becirevic et al., arX iv:hep-lat/9809129.

[16] P . Boucaud, A . Le Yaouanc, J . P . Leroy, J . M icheli, O . Pene and J . Rodriguez-Q uintero, Phys. Lett. B 493 (2000) 315 [arX iv:hep-ph/0008043]; Phys. Rev. D 63 (2001) 114003 [arX iv:hep-ph/0101302]; F . De Soto and J . Rodriguez-Q uintero, Phys. Rev. D 64 (2001) 114003 [arX iv:hep-ph/0105063].

[17] P . Boucaud et al., Phys. Rev. D 66 (2002) 034504 [arX iv:hep-ph/0203119]; Phys. Rev. D 67 (2003) 074027 [arX iv:hep-ph/0208008].

[18] A . E . D orokhov, S . V . E saibegian, A . E . M aximov and S . V . M ikhailov, Eur. Phys. J. C 13 (2000) 331 [arX iv:hep-ph/9903450].

[19] IS . G radshteyn, IM . R yzhik, "Table of Integrals, Series, and Products", Ed. Aca- demic Press., (Sixth ed.) 2000.

[20] J . W . Negele, Nucl. Phys. Proc. Suppl. 73 (1999) 92 [arX iv:hep-lat/9810053].

[21] L . von Smekal, A . Hauck and R . A lkofer, Annals Phys. 267 (1998) 1 [Erratum -ibid. 269 (1998) 182] [arX iv:hep-ph/9707327].

[22] L . von Smekal, R . A lkofer and A . Hauck, Phys. Rev. Lett. 79 (1997) 3591 [arX iv:hep-ph/9705242].

[23] D . Atkinson and J . C . R . Bloch, Phys. Rev. D 58 (1998) 094036 [arX iv:hep-ph/9712459].

[24] D . Atkinson and J . C . R . Bloch, Mod. Phys. Lett. A 13 (1998) 1055 [arX iv:hep-ph/9802239].

[25] J . C . R . Bloch, Few Body Syst. 33, 111 (2003) [arX iv:hep-ph/0303125].

[26] D . Zwanziger, Nucl. Phys. B 364 (1991) 127; Nucl. Phys. B 378 (1992) 525; A . Cucchieri, T . M endes and A . R . Taurines, Phys. Rev. D 67 (2003) 091502 [arX iv:hep-lat/0302022].

[27] M . A . Shifman, A . I . Vainshtein and V . I . Zakharov, Nucl. Phys. B 147 (1979) 385.

[28] S. Narison, Nucl. Phys. Proc. Suppl. 54A (1997) 238 [[arXiv:hep-ph/9609258](https://arxiv.org/abs/hep-ph/9609258)].

[29] V. A. Novikov, M. A. Shifman, A. I. Vainshtein and V. I. Zakharov, Nucl. Phys. B 191 (1981) 301.